

Charge Transfer and Isomerization Reactions of trans-4-(*N*-arylamino)stilbenes

Hsuan-Hsiao Yao,^a Hsu-Hsiang Cheng,^a Cheng-Kai Lin,^b Jye-Shane Yang^{b} and I-*

Chia Chen^{a}*

^a*Department of Chemistry, National Tsing Hua University, Hsinchu, Taiwan 30013,*

Republic of China

^b*Department of Chemistry, National Taiwan University, Taipei, Taiwan 10617,*

Republic of China

Supporting Information: absorption, emission spectra, TCSPC, transient absorption curves and computational results.

Content

- (a) Absorption, emission spectra and Lippert-Mataga plots.
- (b) TCSPC and Transient absorption curves
- (c) Optimized structure, TD-DFT, and MO diagram using method PEB0 basis set 6-311G(d,p)

Captions of Figures and Tables

(a)

Fig. S1. Absorption and fluorescence spectra of p1H, p1CN, and p1OM in various solvents.

Fig. S2. Lippert-Mataga plot of Stokes shift vs. orientation polarizability Δf for p1H.

Fig. S3. Lippert-Mataga plot of Stokes shift vs. orientation polarizability Δf for the (a) PICT, and (b) TICT bands of p1CN.

Fig. S4. Lippert-Mataga plot of Stokes shift vs. orientation polarizability Δf for the PICT band of p1OM.

.

Table S1. Peak positions in absorption λ_{abs} , emission λ_{em} , Stokes shift, and Δf of solvent for p1H in various solvents.

Table S2. Peak positions in absorption λ_{abs} , emission λ_{em} , Stokes shift, and Δf of solvent for p1CN in various solvents.

Table S3. Peak positions in absorption λ_{abs} , emission λ_{em} , Stokes shift, and Δf of solvent for p1OM in various solvents.

(b)

Fig. S5. TCSPC curves measured at emission wavelength 420 nm of p1H in various solvents as indicated.

Fig. S6. TCSPC curves measured at emission wavelength 420 nm of p1CN in various solvents as indicated.

Fig. S7. TCSPC curves measured at emission wavelength 580 nm of p1CN in various solvents as indicated.

Fig. S8. TCSPC curves measured at emission wavelength 420 nm of p1OM in various solvents as indicated.

Fig. S9. TCSPC curves measured at emission wavelength 580 nm of p1OM in various

solvents as indicated.

Fig. S10. Transient absorption spectra of p1H in various solvents as indicated.

Fig. S11. Transient absorption spectra of p1CN in various solvents as indicated.

Fig. S12. Transient absorption spectra of p1OM in various solvents as indicated.

(c)

Fig. S13. Calculated optimized molecular structure of p1H in solvent ACN in the ground state (a) and the PICT state (b).

Table S4. Dihedral angle and energy of p1H in solvent ACN.

Fig. S14. Calculated, optimized molecular structure of p1CN in solvent ACN in the ground state (a), the PICT state (b) and the TICT state (c),(d).

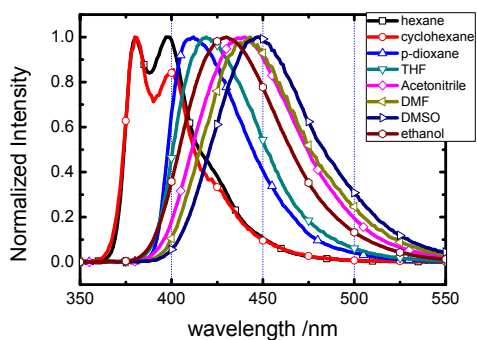
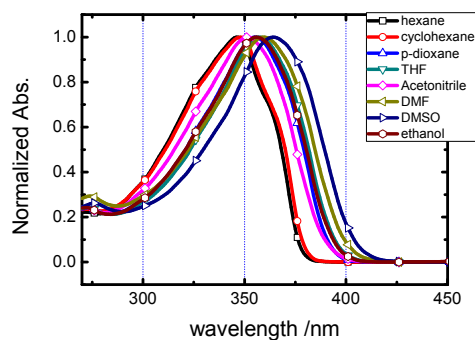
Table S5. Dihedral angle and energy of p1CN in solvent ACN.

Fig. S15. Calculated, optimized molecular structure of p1OM in solvent ACN in the ground state (a), the PICT state (b) and the TICT state (c),(d).

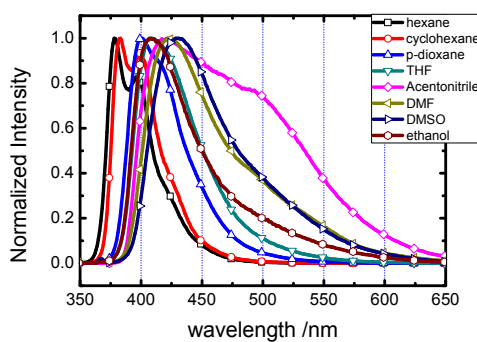
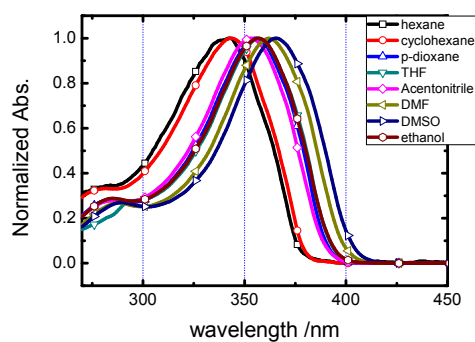
Table S6. Dihedral angle and energy of p1OM in solvent ACN.

Fig. S16. Molecular orbital diagram HOMO, LUMO, and LUMO+1 for p1H, p1CN, and p1OM.

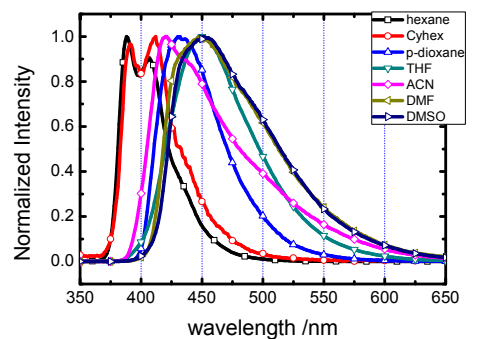
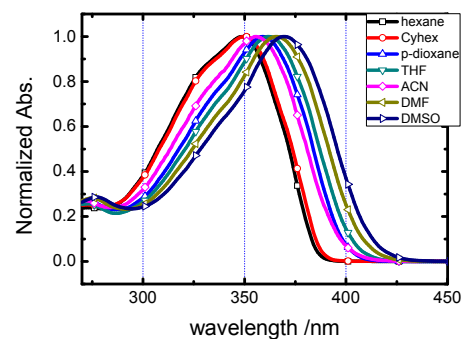
Table S7. Vertical transition (eV) and oscillator strength (in parenthesis) of aminostilbenes in solvent ACN.



p1H



p1CN



p1OM

Fig. S1. Absorption and fluorescence spectra of p1H, p1CN, and p1OM in various solvents.

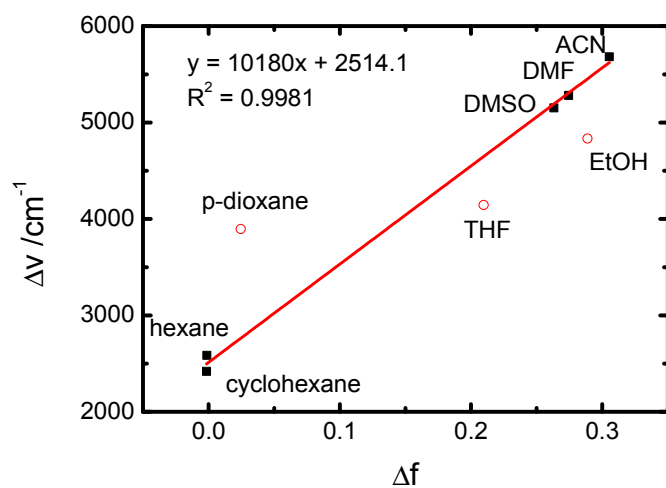


Fig. S2. Lippert-Mataga plot of Stokes shift vs. orientation polarizability Δf for p1H.

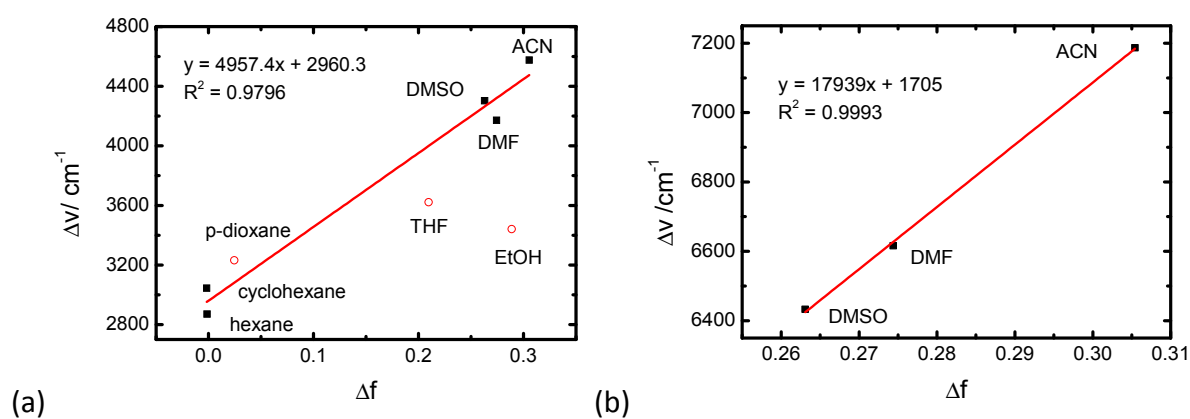


Fig. S3. Lippert-Mataga plot of Stokes shift vs. orientation polarizability Δf for the (a) PICT, and (b) TICT bands of p1CN.

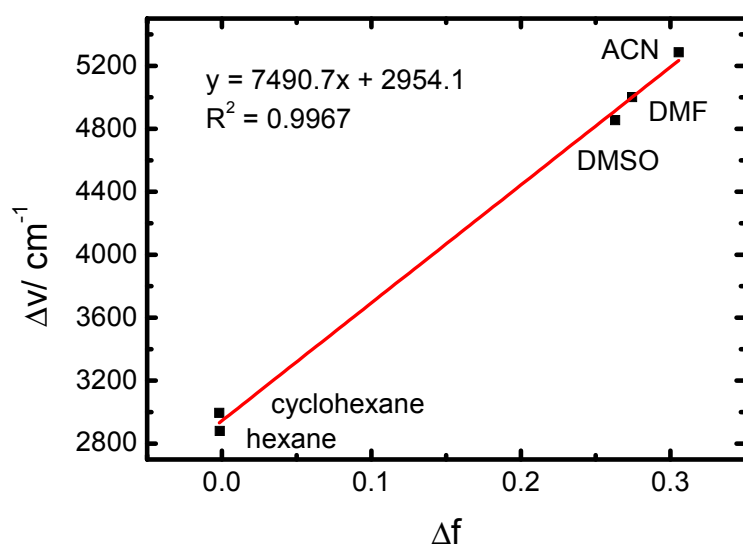


Fig. S4. Lippert-Mataga plot of Stokes shift vs. orientation polarizability Δf for the PICT band of p1OM.

Table S1. Peak positions in absorption λ_{abs} , emission λ_{em} , Stokes shift, and Δf of solvent for p1H in various solvents

solvent	$\lambda_{\text{abs}} / \text{nm}$	$\lambda_{\text{em}} / \text{nm}$	$\nu_{\text{abs}} - \nu_{\text{em}} / \text{cm}^{-1}$	Δf
n-hexane	346	380	2586	-0.00136
Cyclohexane	348	380	2420	-0.00165
p-dioxane	355	412	3897	0.024512
THF	357	419	4145	0.209572
Acetonitrile	352	440	5682	0.305416
DMF	359	443	5282	0.274386
DMSO	364	448	5151	0.263087
EtOH	356	430	4834	0.288746

Table S2. Peak positions in absorption λ_{abs} , emission λ_{em} , Stokes shift, and Δf of solvent for p1CN in various solvents

solvent	$\lambda_{\text{abs}} / \text{nm}$	$\lambda_{\text{em}} / \text{nm}$	$\nu_{\text{abs}} - \nu_{\text{em}} / \text{cm}^{-1}$	Δf
hexane	341	378	2870	-0.00136
cyclohexane	343	383	3045	-0.00165
p-dioxane	355	401	3416	0.024512
THF	357	410	4426	0.209572
Acetonitrile	353	421, 473	4576, 7187	0.305416
DMF	361	425, 476	4171, 6616	0.274386
DMSO	365	433, 477	4303, 6433	0.263087
EtOH	357	407	3441	0.288746

Table S3. Peak positions in absorption λ_{abs} , emission λ_{em} , Stokes shift, and Δf of solvent for p1OM in various solvents^a

solvent	$\lambda_{\text{abs}} / \text{nm}$	$\lambda_{\text{em}} / \text{nm}$	$\nu_{\text{abs}} - \nu_{\text{em}} / \text{cm}^{-1}$	Δf
hexane	350	388	2880	-0.00136
cyclohexane	349	391	2996	-0.00165
p-dioxane	359	432	4707	0.024512
THF	362	450	5402	0.209572
Acetonitrile	355	420	5286	0.305416
DMF	366	449	5001	0.274386
DMSO	370	451	4854	0.263087
EtOH	359	444	5332	0.288746

a. The Stokes shift is for the PICT band and the TICT band position is hard to determine.

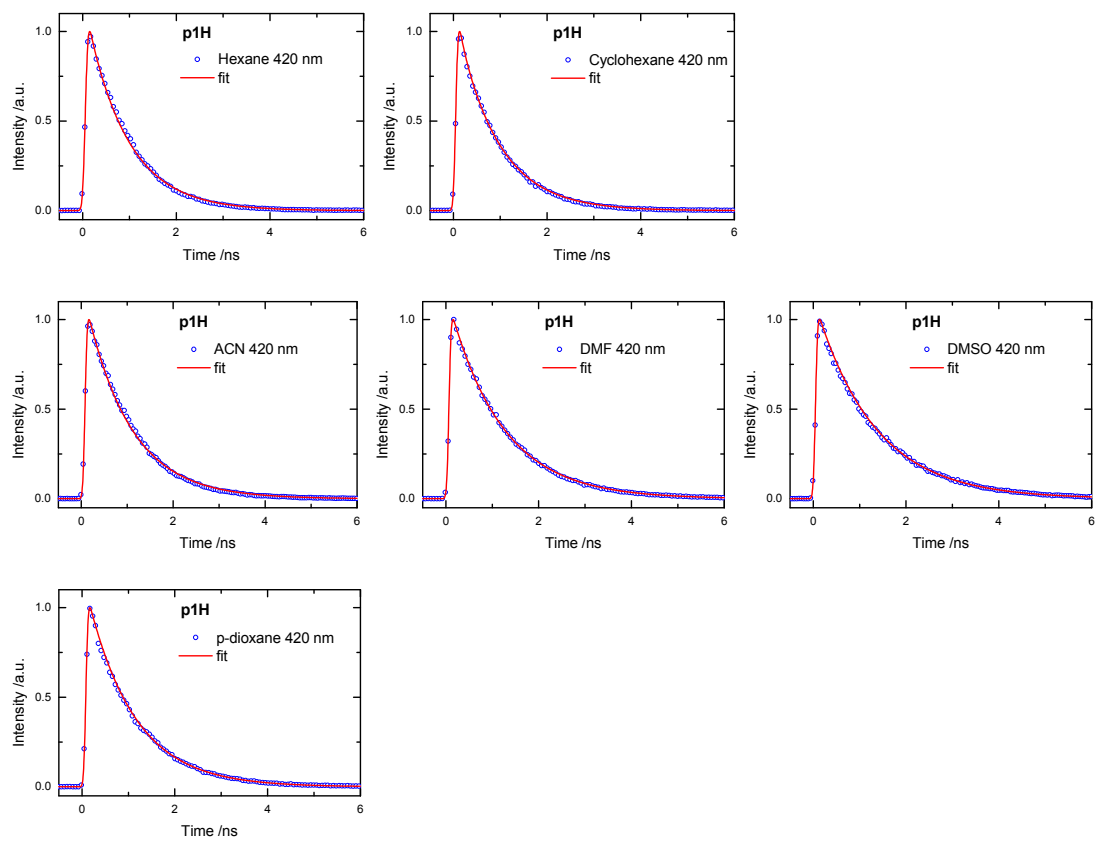


Fig. S5 TCSPC curves measured at emission wavelength 420 nm of p1H in various solvents as indicated

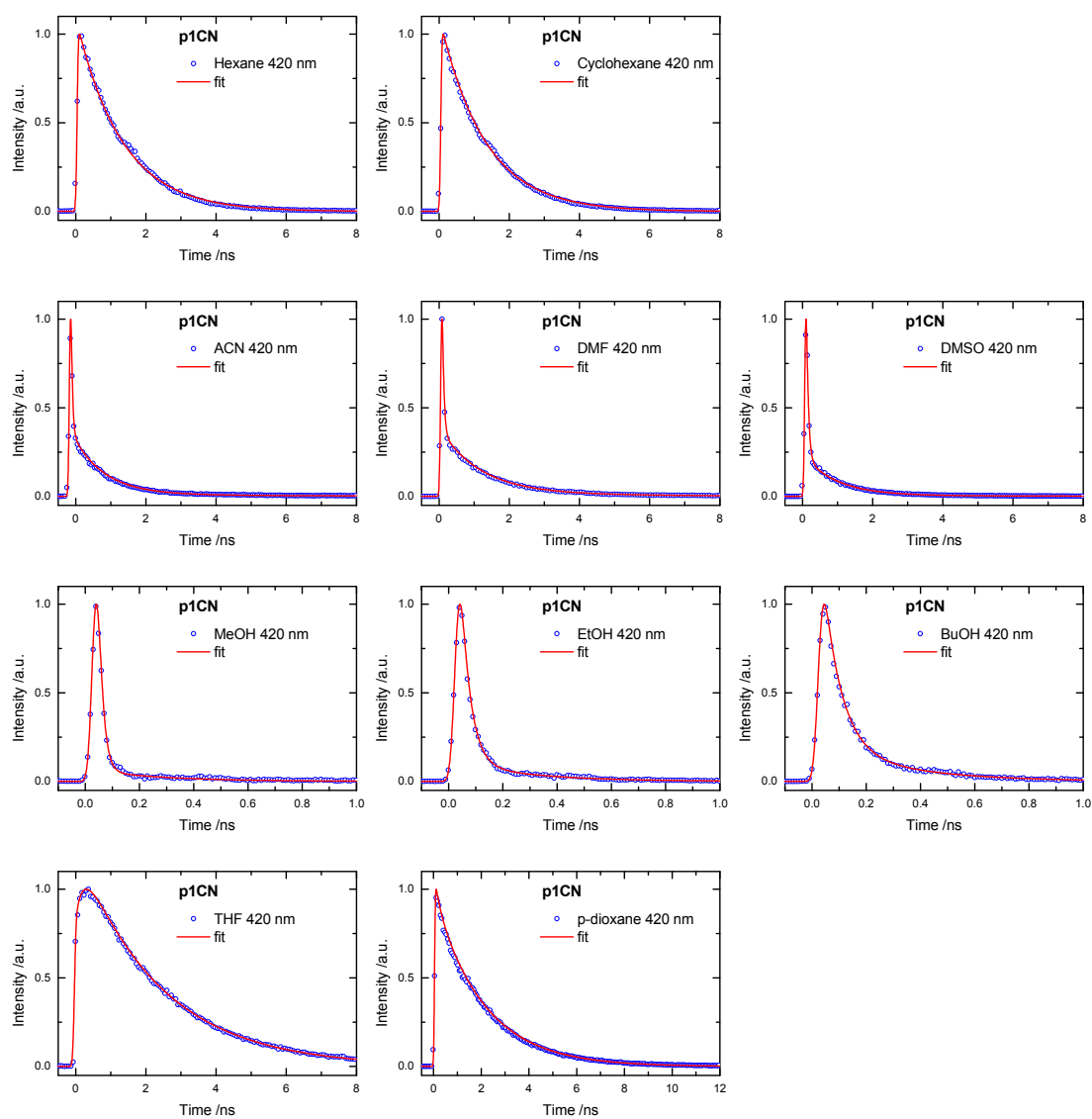


Fig. S6 TCSPC curves measured at emission wavelength 420 nm of p1CN in various solvents as indicated

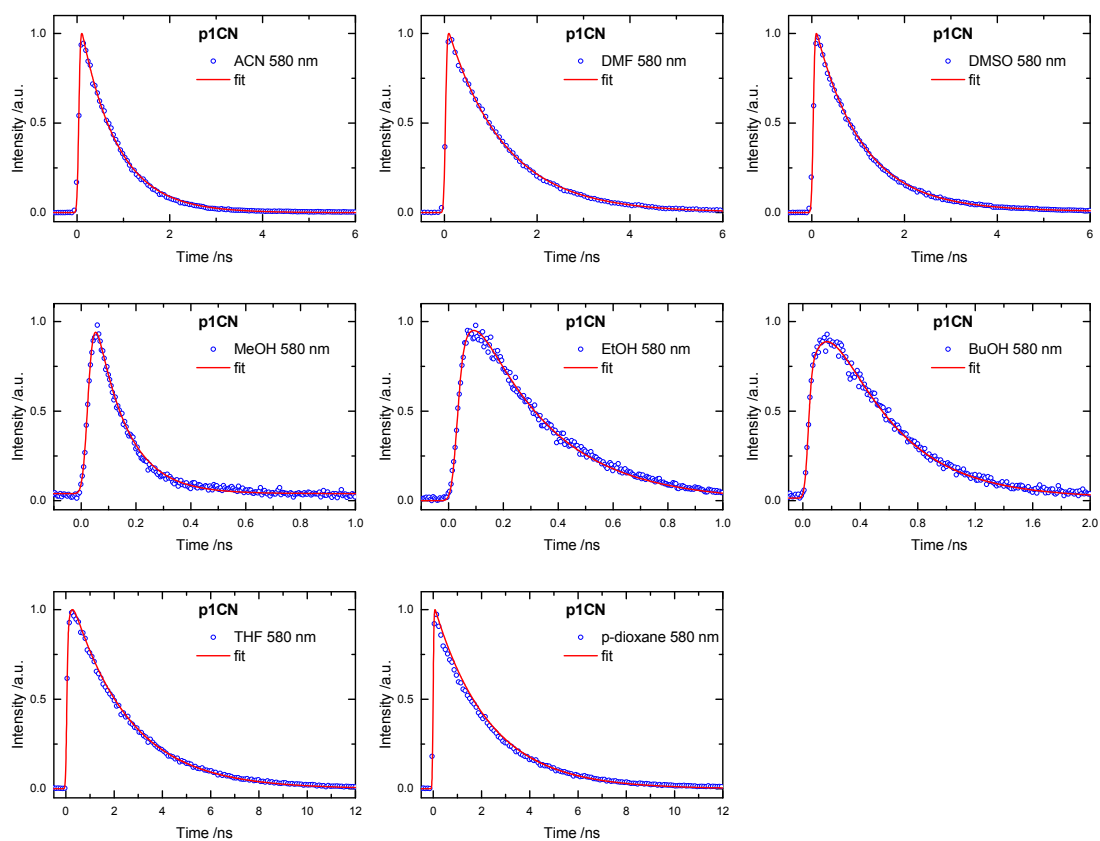


Fig. S7 TCSPC curves measured at emission wavelength 580 nm of p1CN in various solvents as indicated

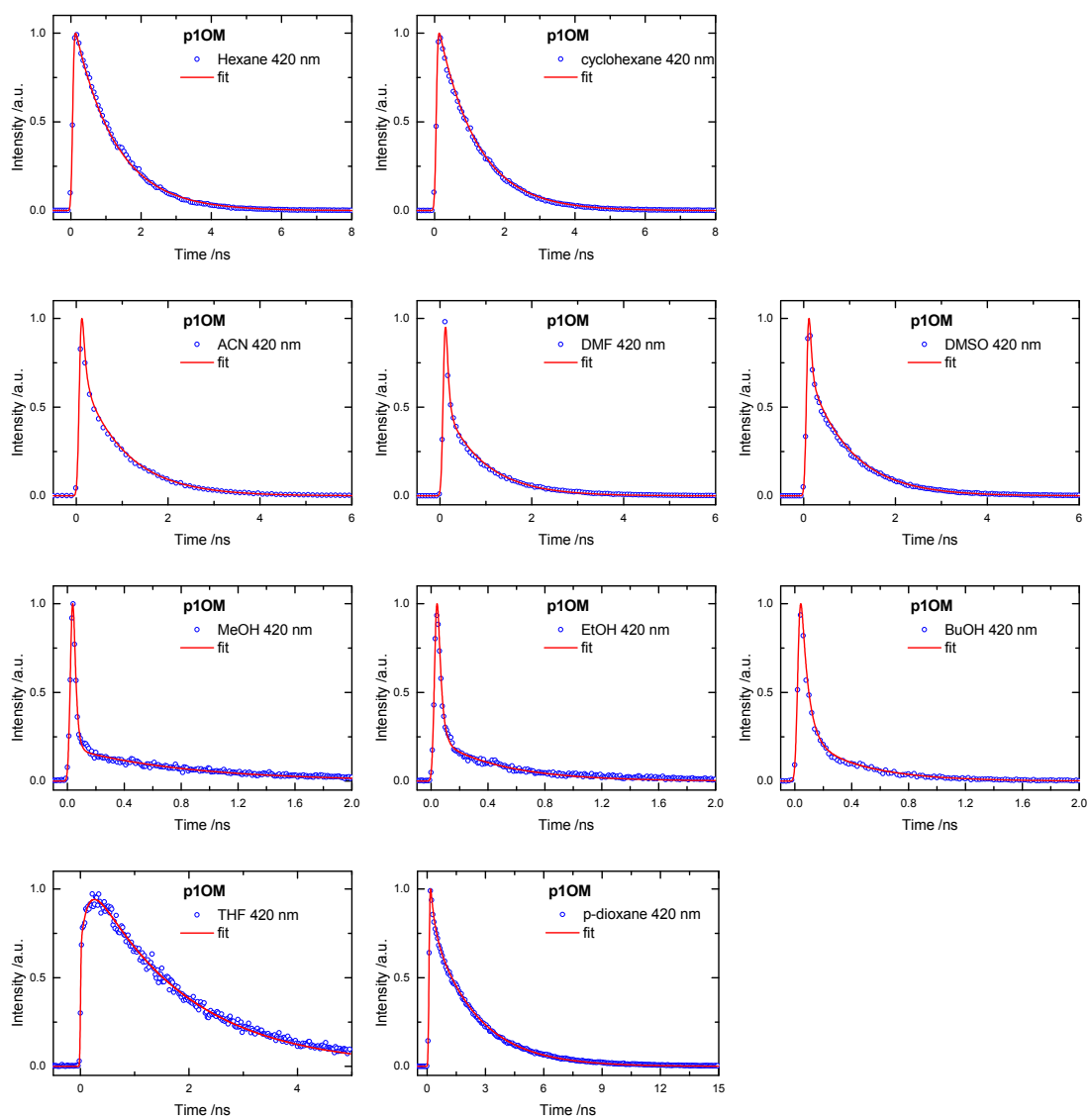


Fig. S8 TCSPC curves measured at emission wavelength 420 nm of p1OM in various solvents as indicated

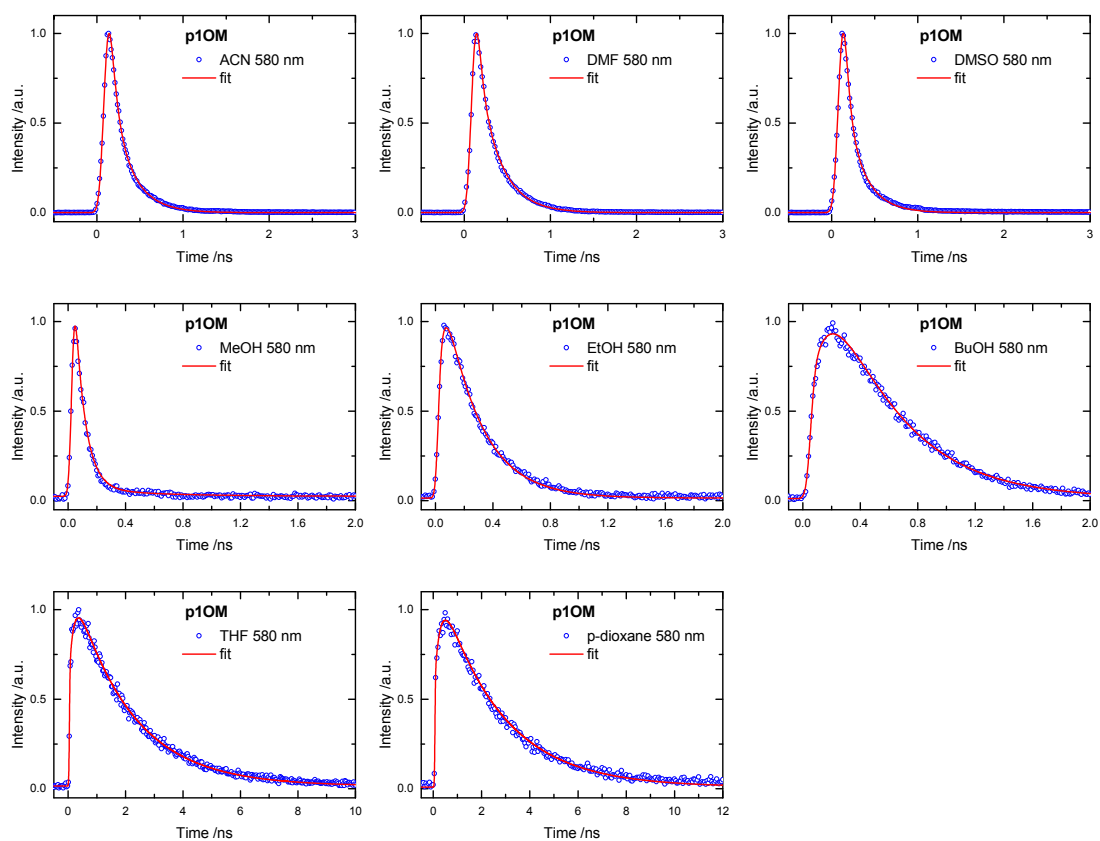


Fig. S9 TCSPC curves measured at emission wavelength 580 nm of p1OM in various solvents as indicated

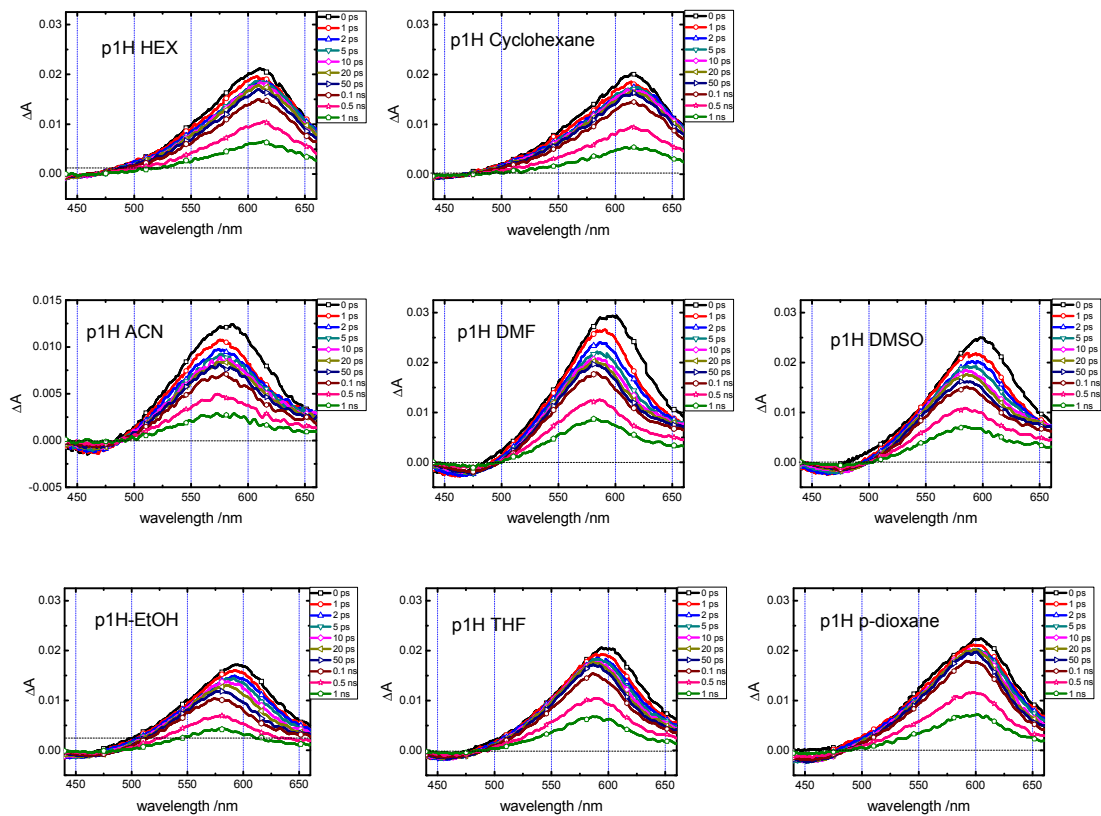


Fig. S10 Transient absorption spectra of p1H in various solvents as indicated.

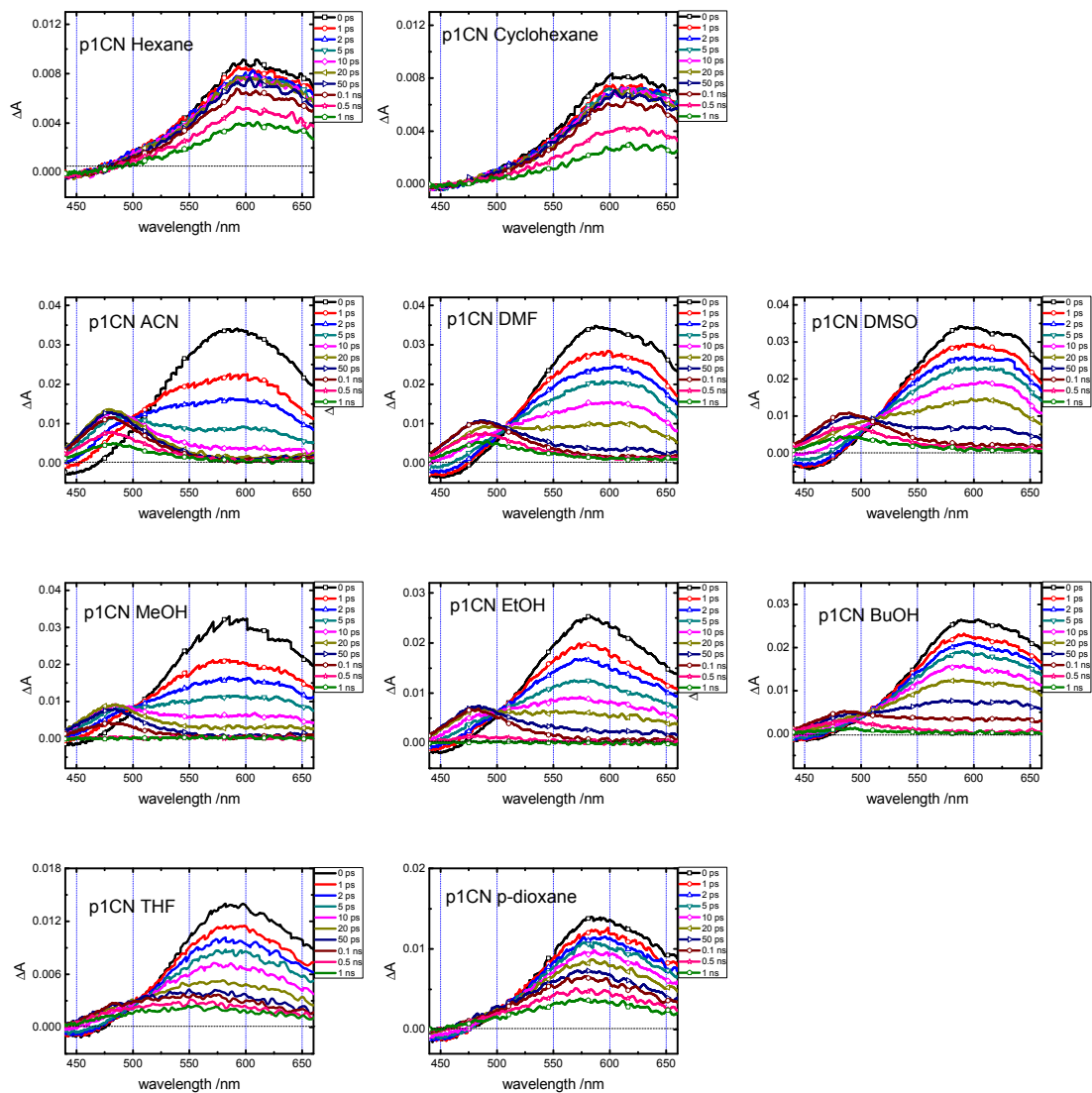


Fig. S11 Transient absorption spectra of p1CN in solvent as indicated

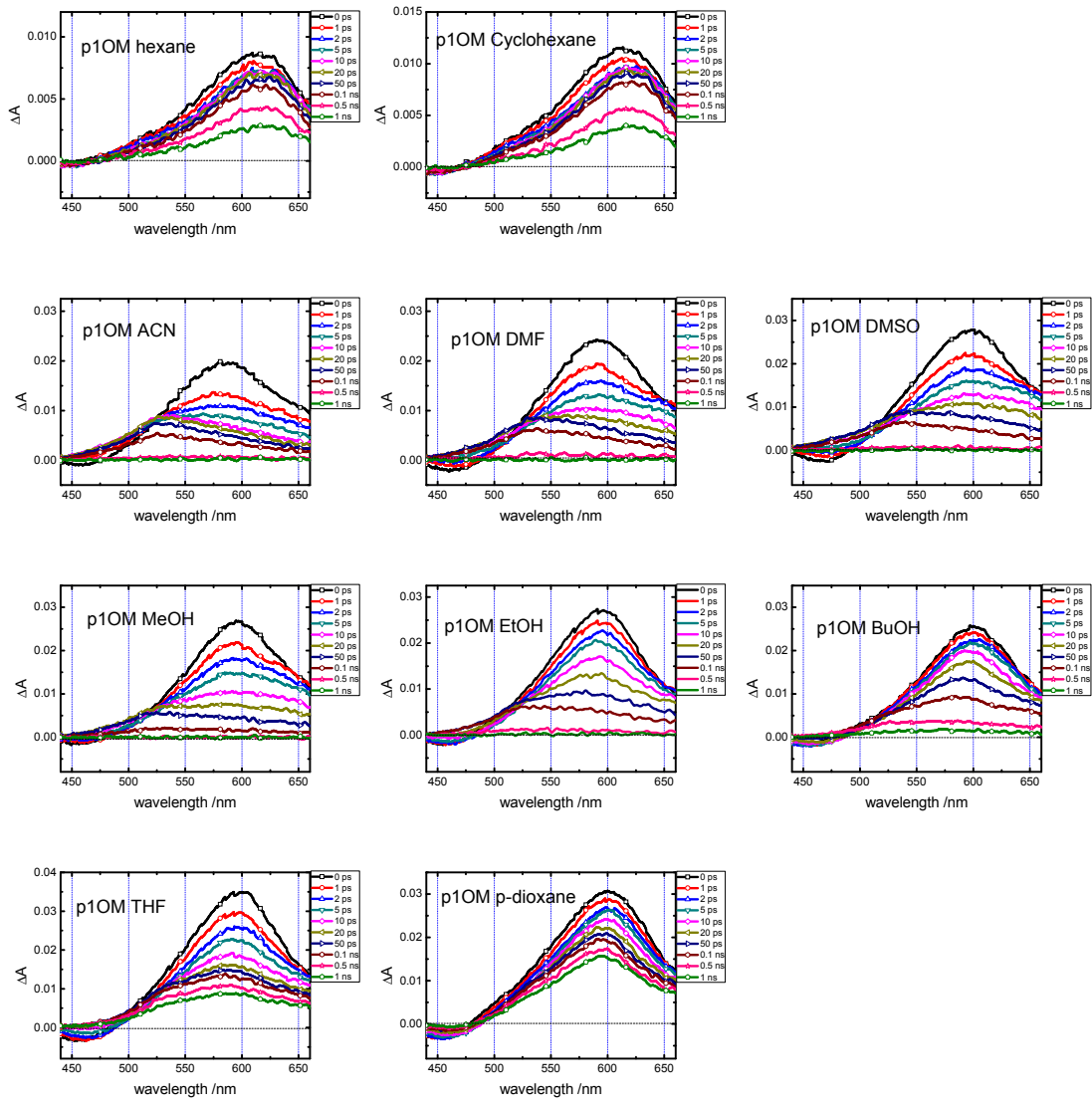


Fig. S12 Transient absorption spectra of p1OM in various solvents as indicated

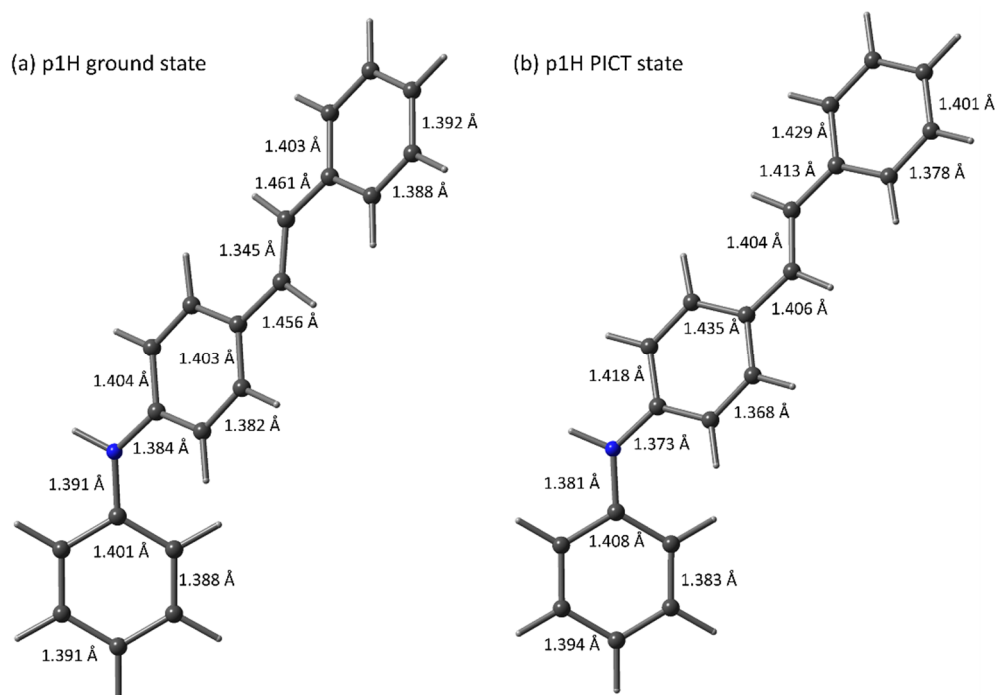


Fig. S13 Calculated optimized molecular structure of p1H in solvent ACN in the ground state (a) and the PICT state (b).

Table S4 Dihedral angle and energy of p1H in solvent ACN.

state	ground state	PICT
$\varphi_{\text{stilbene-aniline}}$	41°	40°
$\varphi_{\text{NH-aniline}}$	22°	21°
$\varphi_{\text{NH-stilbene}}$	20°	20°
energy (eV)	0	3.09

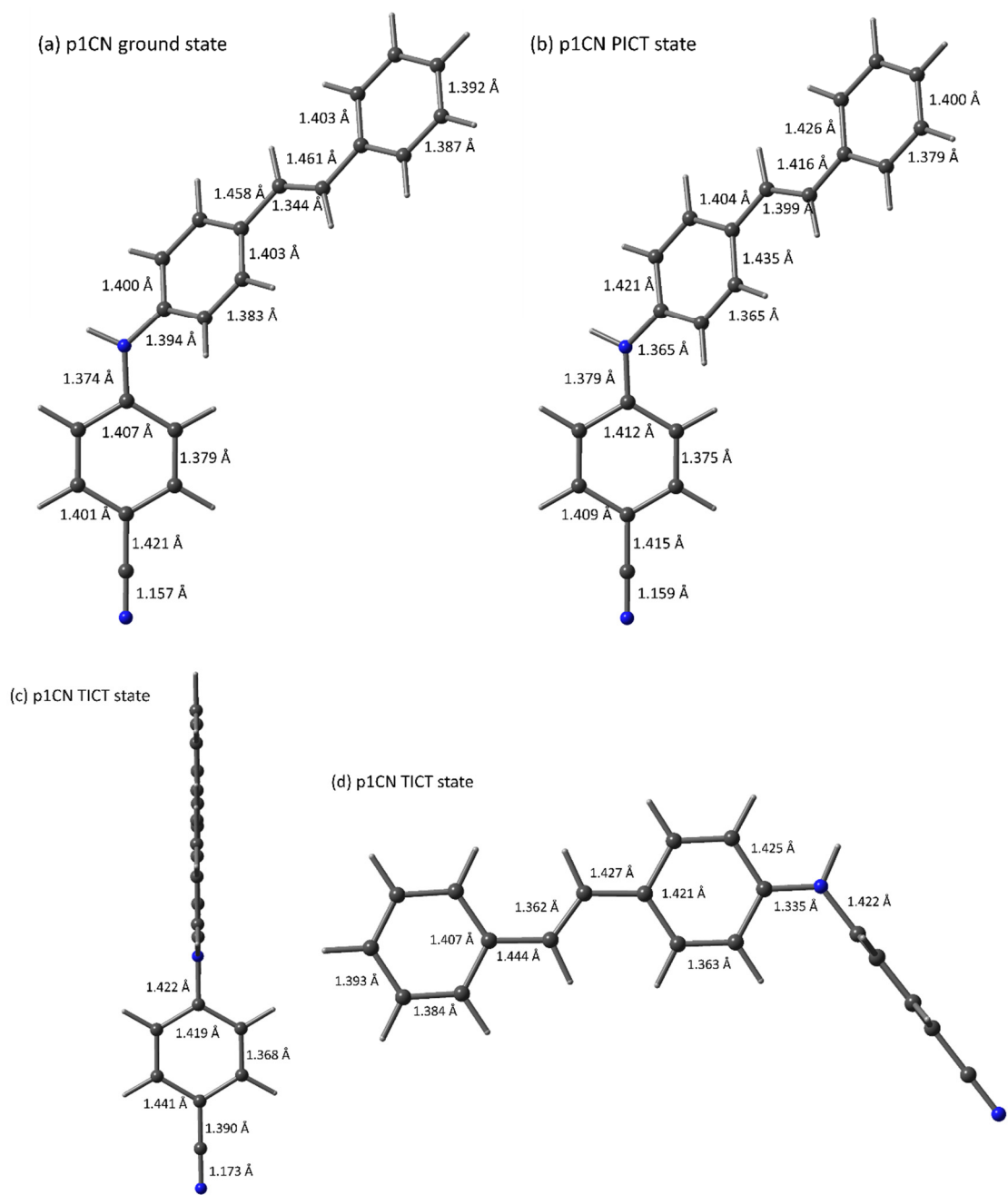
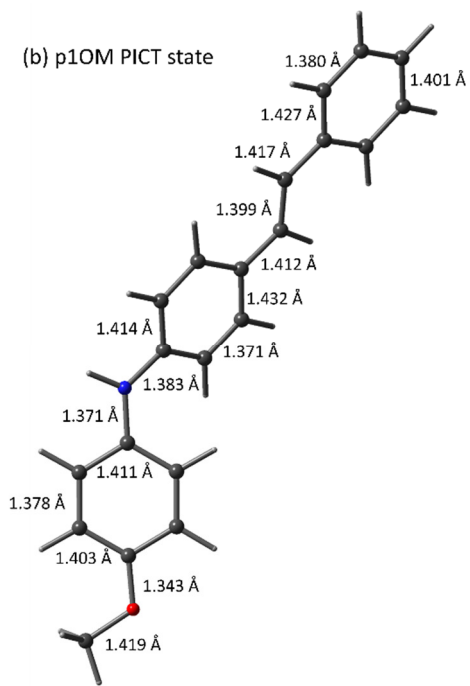
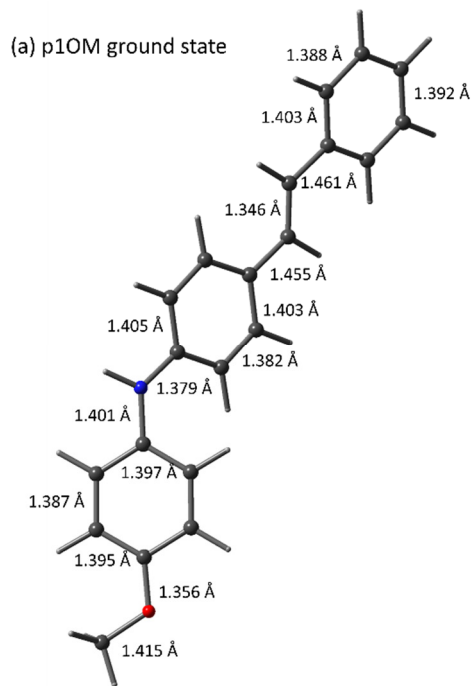


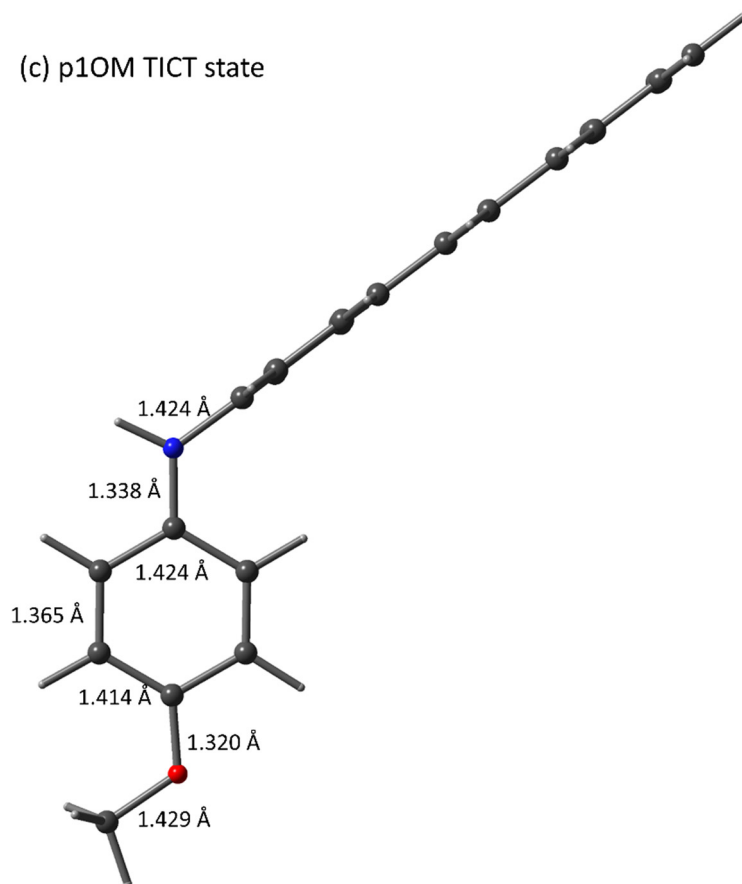
Fig. S14 Calculated, optimized molecular structure of p1CN in solvent ACN in the ground state (a), the PICT state (b) and the TICT state (c),(d).

Table S5 Dihedral angle and energy of p1CN in solvent ACN..

state	ground state	PICT	TICT
$\varphi_{\text{stilbene-aniline}}$	42°	38°	90°
$\varphi_{\text{NH-aniline}}$	16°	22°	89°
$\varphi_{\text{NH-stilbene}}$	26°	17°	0°
energy (eV)	0	3.13	2.78



(c) p1OM TICT state



(d) p1OM TICT state

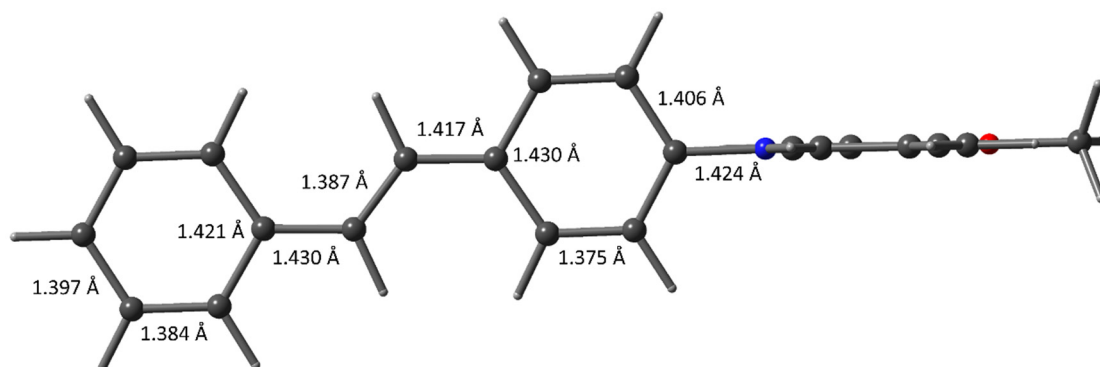


Fig. S15 Calculated, optimized molecular structure of p1OM in solvent ACN in the ground state (a), the PICT state (b) and the TICT state (c),(d).

Table S5 Dihedral angle and energy of p1OM in solvent ACN.

	ground state	PICT	TICT
$\varphi_{\text{stilbene-aniline}}$	46°	42°	84°
$\varphi_{\text{NH-aniline}}$	29°	18°	1°
$\varphi_{\text{NH-stilbene}}$	17°	25°	83°
energy (eV)	0	2.77	1.88

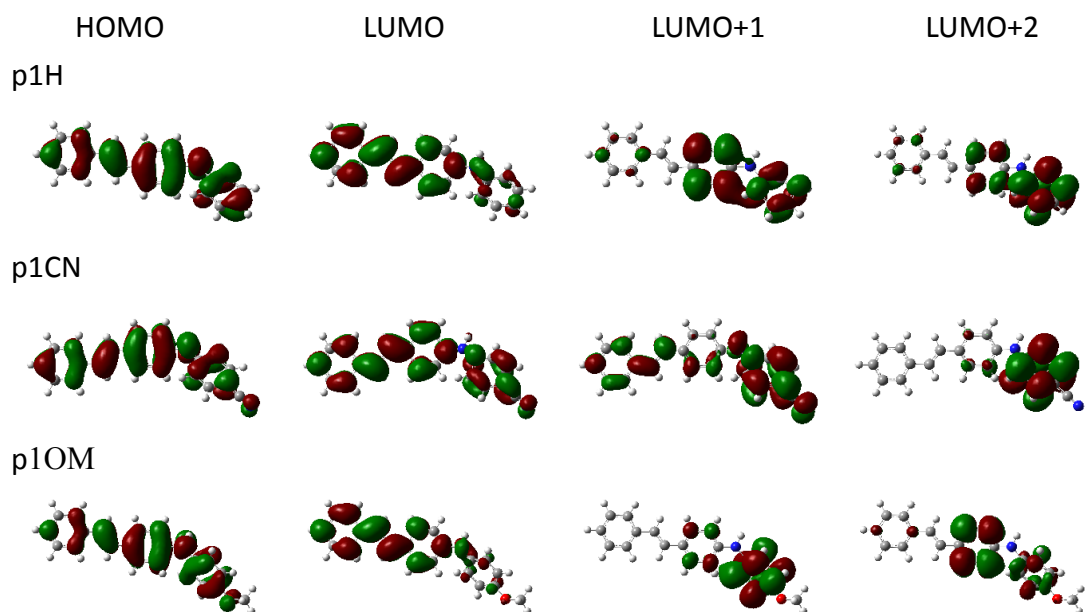


Fig. S16 Molecular orbital diagram HOMO, LUMO, LUMO+1 and LUMO+2 for p1H, p1CN, and p1OM.

Table S7 Vertical transition (eV) and oscillator strength (in parenthesis) of aminostilbenes in solvent ACN.

	p1H	p1CN	p1OM
S1 (HOMO→LUMO)	3.3014 (1.1944)	3.3827 (1.4325)	3.1950 (1.1288)
S2 (HOMO→LUMO+1)	4.2037 (0.0242)	4.1501 (0.0741)	4.0883 (0.0149)
S3 (HOMO→LUMO+2)	4.3247 (0.0208)	4.2889 (0.0175)	4.1857 (0.0176)